Lawrence Berkeley National Laboratory
LBL Publications

Title
TEM Studies of Carbon Coated LiFePO4 after Charge Discharge Cycling

Permalink
https://escholarship.org/uc/item/8fp0x9vs

Authors
Gabrisch, H.
Wilcox, J.
Doeff, M.

Publication Date
2007

TEM Studies of Carbon Coated LiFePO$_4$ after Charge Discharge Cycling

H. Gabrisch[a], J. Wilcox[b], and M. Doeff[b]

[a] Department of Chemistry, University of New Orleans, New Orleans, LA 70148
[b] Division of Materials Science, Lawrence Berkeley National Laboratory, Berkeley, CA 94720

Carbon coating has proven to be a successful approach to improve the rate capability of LiFePO$_4$ used in rechargeable Li-ion batteries. Investigations of the microstructure of carbon coated LiFePO$_4$ after charge discharge cycling shows that the carbon surface layer remains intact over 100 cycles. We find micro cracks in the cycled material that extend parallel to low indexed lattice planes. Our observations differ from observations made by other authors. The differences between the orientations of crack surfaces in both studies can be reconciled considering the location of weak bonds in the unit cell and specimen geometry as well as elastic stress fields of dislocation.

Introduction

LiFePO$_4$, first introduced by Padhi et al, is considered a promising low cost, environmentally benign cathode material for application in batteries for electric and hybrid vehicles (1). The removal of Li from LiFePO$_4$ proceeds via a two phase reaction in which heterosite (FePO$_4$) forms directly from the fully lithiated tryphilite LiFePO$_4$. LiFePO$_4$ and the delithiated FePO$_4$ belong to the group of phospho-olivines. The orthorhombic unit cell (SG 62, Pnma symmetry) consists of a distorted hexagonal close packed stacking of oxygen into which octahedrally coordinated Fe and Li ions and tetrahedrally coordinated P-ions are embedded. The migration of Li-ion takes place parallel to the b direction in tunnels between FeO$_6$ octahedra and PO$_4$ tetrahedra (2). The unit cell dimensions are a=10.33Å, b= 6.01Å, c= 4.69Å for LiFePO$_4$ and a=9.76Å, b=5.75Å, c=4.76Å for FePO$_4$. The change in unit cell volume when going from tryphilite to the heterosite amounts to approximately 6.8%, which induces a considerable amount of stress at the two phase interface (3). Despite its high theoretical capacity of 170 mAh/g a major obstacle to the commercialization of LiFePO$_4$ is its poor electronic conductivity that limits achievable discharge rates (1). Reduction in particle size (4), carbon coating (5-7) and addition of small metallic particles (8) are among the approaches used to enhance the electrochemical performance of LiFePO$_4$. We successfully employed carbon coating with pyromellitic acid and ferrocene to enhance the rate capability of electrodes based on LiFePO$_4$ (9). Studies of the virgin material by Energy Filtered Imaging (EFTEM) showed that a carbon layer thickness of about 10 nm is sufficient to improve the electrochemical behavior (10).

In the original paper Padhi introduced a simplified core shell model for the distribution of the two phases (1). The highly anisotropic unit cell of LiFePO$_4$ and the resulting preferred direction of Li diffusion however raise concerns about the validity of the core shell model. Recently Chen et al. investigated LiFePO$_4$ before and after chemical delithiation by transmission electron microscopy (11). In Li$_{0.5}$FePO$_4$ the authors found regions of alternating contrast that were sometimes separated by cracks with (100)

surface planes. A high resolution image taken from a thin region near a crack suggests that stripes of LiFePO$_4$ and FePO$_4$ extend parallel to (100) planes. The finding of alternating FePO$_4$ and LiFePO$_4$ zones was qualitatively confirmed by a high resolution electron energy loss study (12) reviving the debate about the location of the LiFePO$_4$/FePO$_4$ interface.

Here we report the results of investigations by Transmission Electron Microscopy on carbon coated LiFePO$_4$ particles retrieved from cycled electrodes. We found cracks similar to those observed after chemical delithiation. However a major difference exists in the orientation of the crack surfaces. We consider the geometry of crack formation in LiFePO$_4$ based on dislocation glide systems and compare the orientation of cracks found in our material to observations made on LiFePO$_4$ synthesized by a hydrothermal route (11).

Experimental

LiFePO$_4$ was synthesized by a sol gel method using iron nitrate, lithium acetate, phosphoric acid and glycolic acid precursors as detailed in reference (9). After initial firing at 500°C to decompose these precursors, 6wt% pyromellitic acid and 1wt% ferrocene was added and the mixture was subsequently fired to 600ºC for 10 hours under N$_2$ atmosphere. Laminated electrodes containing 80 wt % active material, 8 wt % Kynar poly(vinylidene fluoride), 6 wt % SFG-6 synthetic flake graphite, and 6 wt % compressed acetylene black were prepared. Electrodes were punched out to 1.8 cm^2 size, with loadings of about 5-10 mg/cm^2 active material. 2032 size coin cells were assembled in a helium-filled glove box, using lithium metal as a counter electrode and 1 M LiPF$_6$ in 1:2 ethylene carbonate/dimethyl carbonate (EC/DMC) as the electrolytic solution. Cells were cycled galvanostatically between 2.0 and 3.9V using a MacPile II potentiostat/galvanostat. All cells were charged at C/25 rate, and discharged at either C/25 (cell 1) or C/2 (cell 2) rates. The cycling behavior of the two cells varied as shown in Fig.1. At the lower discharge rate of C/25 about 145 mAh/g was retrieved from the cathode per discharge with no apparent decline in performance over the range of the experiment. At the higher discharge rates used in cell 2, a smaller specific
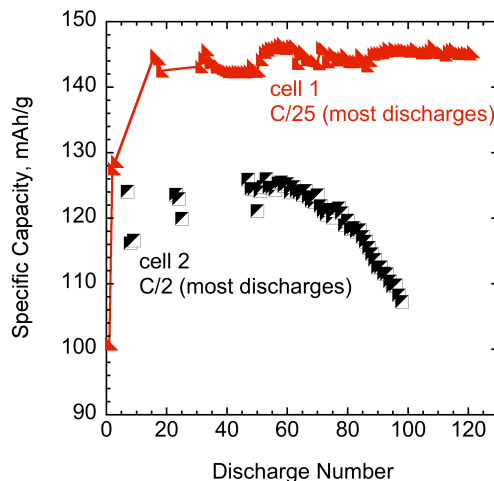

Figure 1 : Comparison of the specific capacities observed at discharge rates C/25 and C/2.

capacity of 125mAh/g is observed that begins to deteriorate after about 50 charge-discharge cycles. The cells were stopped after approximately 100 charge discharge cycles and disassembled. The graphite/binder/powder mixture was scraped off the Al collectors and washed repeatedly in NMP to dissolve the binder followed by a wash in acetone. The particle/acetone solution was dispersed on a holey carbon grid to prepare TEM specimens. For comparison, $Li_{0.5}FePO_4$ obtained by chemical delithition of $LiFePO_4$ produced by a hydrothermal method (11) was also studied. TEM investigations were performed on a JEOL 3010 at the National Center for Electron Microscopy in Berkeley and the JEOL 2010 at the University of New Orleans. Both microscopes were operated at 200kV. Experimental electron diffraction patterns were compared to electron diffraction patterns simulated with the software packet Desktop Microscopist using unit cells published in literature (3).

Results

No qualitative microstructural differences were observed between particles retrieved from cell 1 and cell 2. The most prominent feature observed in the cycled particles is the formation of large cracks parallel to low indexed lattice directions. The cracks start at the specimen surface and extend into the interior of the particle. An example from a particle retrieved from cell 1 is shown in Fig. 2 together with the corresponding diffraction pattern. The orientation of the crack surface is parallel to (010) lattice planes. Close examination of the particle surface in specimens from both electrodes showed that the carbon surface layer has remained intact over more than 100 charge discharge cycles. Fig. 3 shows an example of a particle in [011] orientation demonstrating homogeneous layer thickness over a wide range of particle surface orientations. A close look at the selected area diffraction patterns in Fig. 2b and Fig 3b shows that spot splitting can be observed on diffraction spots further away from the incident beam (see arrow). The small separation of the spots is typical for the small difference in lattice parameters between
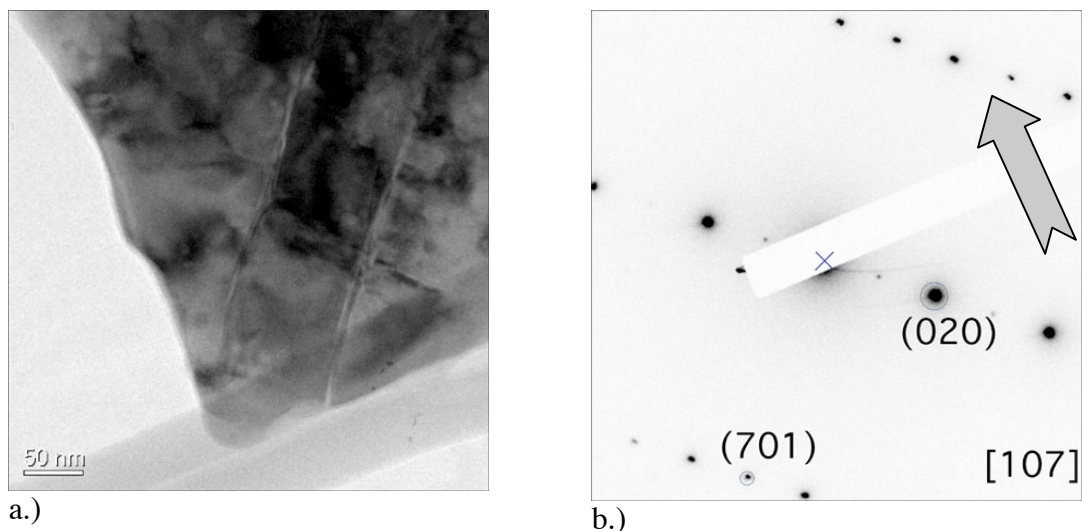

a.)   b.)

Figure 2 : Image showing cracks parallel to (010) planes and corresponding diffraction pattern taken from a $LiFePO_4$ particle retrieved from cycled cell. Cracks are observed repeatedly in particles retrieved from cycled cell 1 and 2.

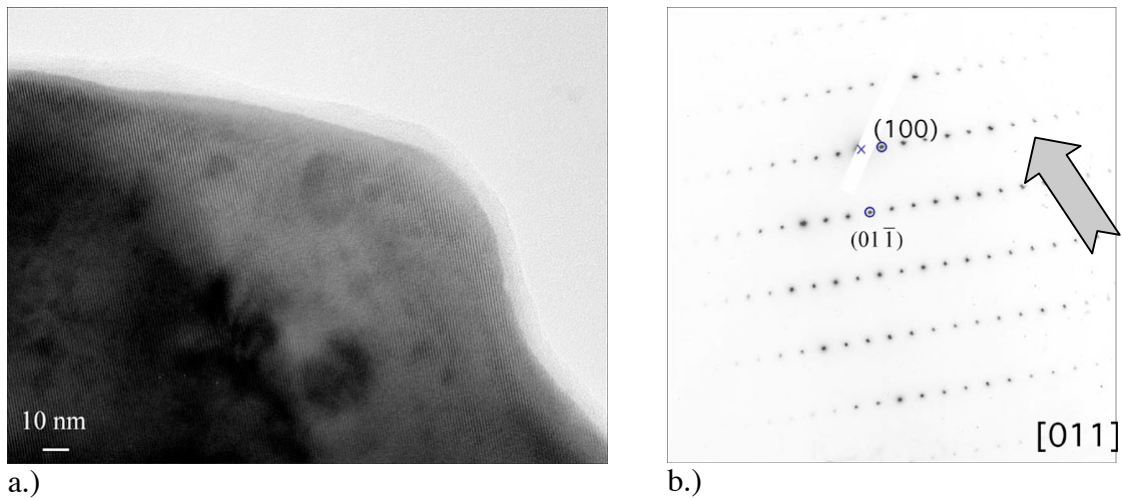a.)   b.)

Figure 3 : Carbon surface layers on cycled particles show no damage or orientation dependence of layer thickness (cycled cell 1).
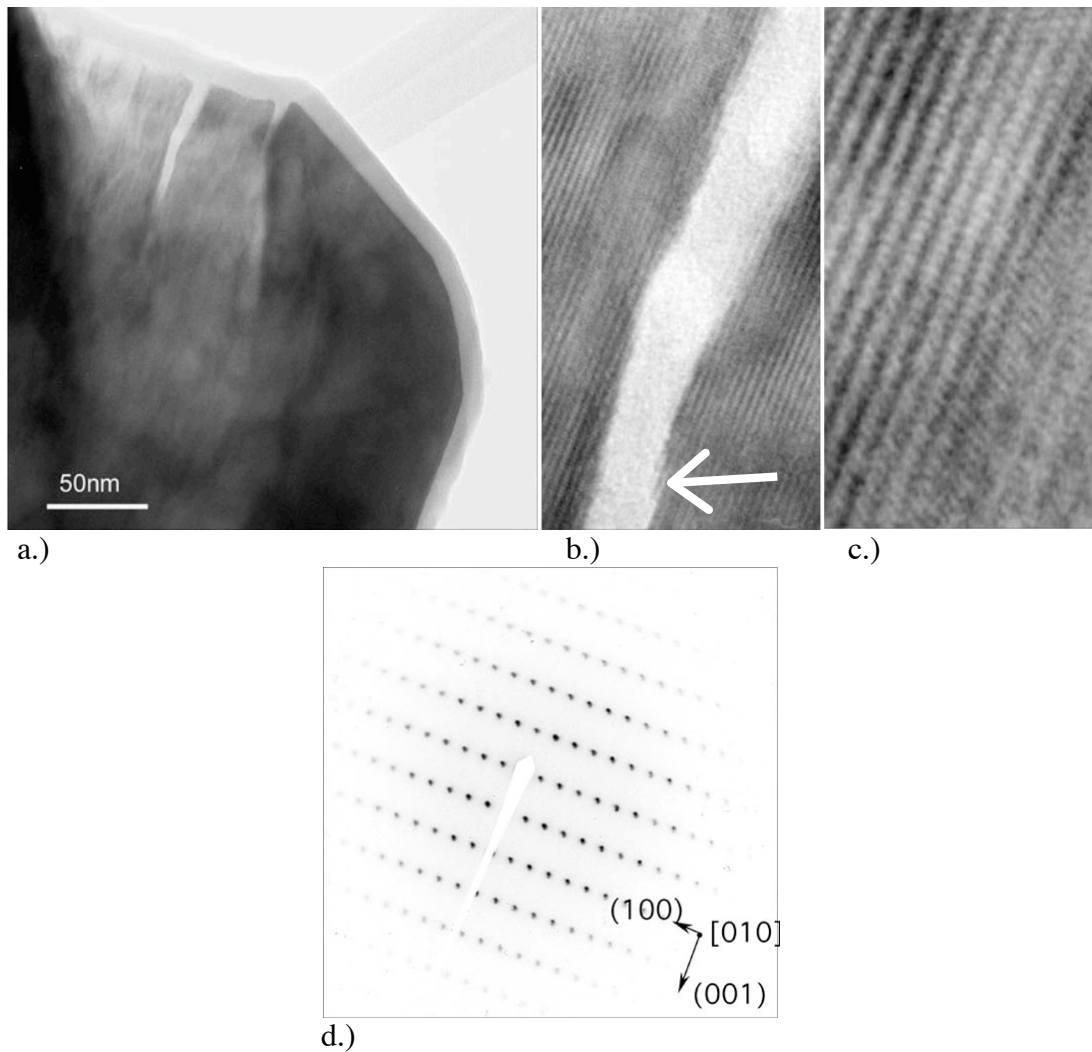

a.)   b.)   c.)

d.)

Figure. 4 : Image (a.) and diffraction pattern (d.) taken from $Li_{0.5}FePO_4$ synthesized from hydrothermally produced $LiFePO_4$. The crack surface is oriented parallel to (100) planes. The enlarged section in b. shows that the crack surface extends over several lattice planes (see arrow). Further enlargement in c. shows that twinning or stacking faults are present in the material.

closely related phases like LiFePO$_4$ and FePO$_4$. The analysis of single crystal electron diffraction patterns taken from the cycled and from the as synthesized material showed that no preferred particle orientation could be found in the prepared TEM specimens.

Fig. 4a shows a micrograph from chemically delithiated Li$_{0.5}$FePO$_4$. Cracks similar to the ones observed after charge discharge cycling were observed. However in these specimens the orientation of the crack surface is parallel to (100) planes as can be seen from a comparison to the diffraction pattern shown in Fig. 4d. A magnified view of the crack surface in Fig.4b shows that the materials separation is not clear cut between two lattice planes. Instead the crack surface extends over several lattice planes as indicated by an arrow in Fig. 4b. Further enlargement of the area near the crack surface in Fig. 4c shows a change of the image contrast that indicates presence of twins or stacking faults in this area. Imaging of a delithiated particle in 2 beam condition shows a concentration of strain along lines that are parallel to [101] directions in the plane of the particle, see Fig. 5. The particles synthesized by the hydrothermal method have a plate like shape with the [010] direction parallel to the surface normal of the particle.
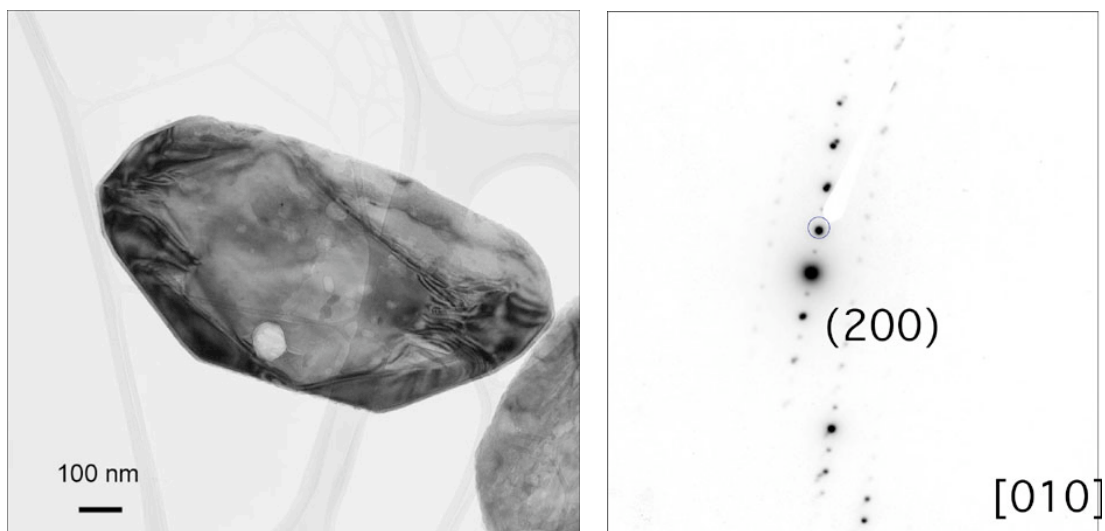

Figure 5 : Li$_{0.5}$FePO$_4$ imaged with diffraction intensity originating from (020) planes. The dark lines lying diagonally in the particle plane indicate presence of stress in the surrounding regions. The line directions are approximately parallel to [101] directions.

Discussion

The finding that the carbon surface layer withstands charge discharge cycling over many cycles without any visible damage or alterations is encouraging for future practical implementation of the coating method used in this study. The presence of micro cracks in particles retrieved from both cathodes suggests that these features are not responsible for the observed difference in electrochemical behavior. This is in contrast to a finding published in (13) where observed capacity loss is attributed to crack formation. In order to fully eliminate crack formation as a factor affecting electrochemical behavior a more quantitative investigation of the number of cracks observed in particles from either cathode is needed.

The different orientations of crack surfaces observed in cycled powders produced by sol gel method and in chemically delithiated powders produced hydrothermally is a disturbing result that asks for an explanation. We looked at the building blocks of the

microstructure to understand how the breaking of bonds between the building blocks of this structure can explain both observations. In a second approach we estimate the order of elastic stresses in the material that needs to be overcome to form cracks by dislocation glide.

Fig. 6 shows schematic drawings of the olivine structure projected into the (001) plane (Fig. 6a) and into the (100) plane (Fig. 6b). Fig. 6a shows how sheets of edge sharing FeO_6 octahedra (shaded brown) form (100) planes that are connected in [100] direction by PO_4 tetrahedra (shaded grey). The bond between two (100) planes is where the corners of PO_4 tetrahedra and FeO_6 octahedra meet- making this a weak bond which explains the formation of cracks between (100) planes. A plan view of a (100) plane in Fig. 6b shows that the sheets of edge sharing FeO_6 octahedra (shaded red) are better described by serrated chains of edge sharing FeO_6 octahedra parallel to the [100] direction. In [010] direction these chains are connected by PO_4 tetrahedra that extend above and below the plane of the drawing (shaded yellow and blue respectively). Hence the formation of cracks between (010) planes can proceed by breaking of the same type of bonds between FeO_6 and PO_4 corners as in the case of breaking between (100) planes. A more quantitative view is to consider actual stresses that need to be overcome in order to create a crack by a dislocation glide mechanism.
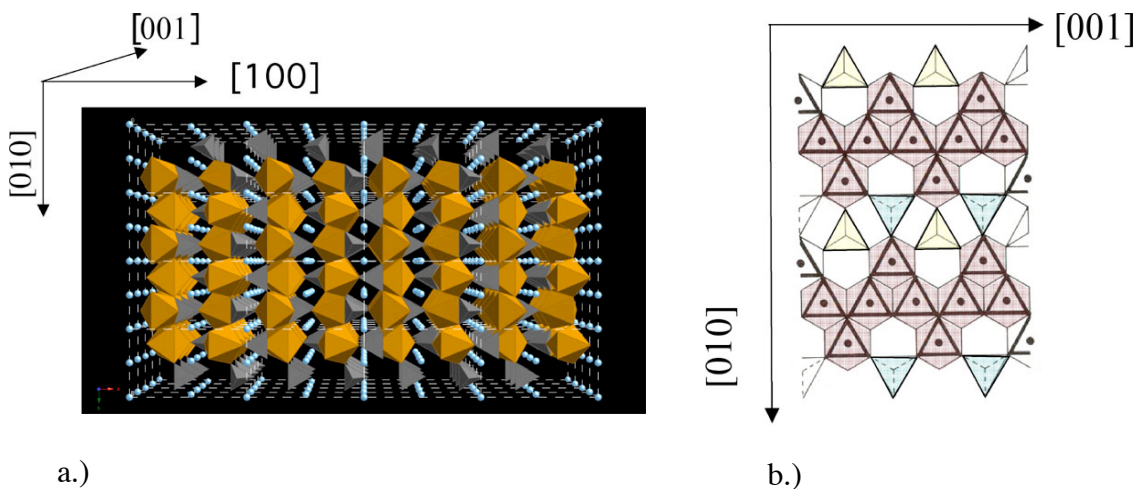

a.)   b.)

Figure 6 : Arrangement of PO_4 tetrahedra and FeO_6 octahedra in $LiFePO_4$ seen in the (001) plane (a.) and in the (100) plane (b.)

Dislocations are one dimensional lattice defects that can be described by a deviation of actual atom positions from their assigned lattice sites. The movement of such a defect through the volume of a specimen is a mechanism of plastic deformation. Another mode of deformation is twinning (not considered here). The magnitude and direction of the atom displacement caused by the presence of a dislocation is described by the Burgers vector $\vec{b}$, for example $\vec{b}$=[100] describes a displacement in [100] direction by the length of one lattice constant in that direction (a=10.33Å). For comparison the lengths of Burgers vectors in [010] and [001] direction are 6.01Å and 4.7Å respectively. Displacement along different directions and in different planes (glide planes) will cause cracks in different directions. The combination of a Burgers vector and a glide plane is called a slip system. Table I compares the slip systems that can lead to formation of cracks having (100) and (010) surface planes. Notice that a dislocation with the Burgers vector [001] is glissile in both the (100) and the (010) plane.

Table I : Slip systems for formation of (100) and (010) cracks.	
glide in (100) plane	**glide in (010) plane**
(100) [010]	(010) [100]
(100) [001]	(010) [001]
(100) [011]	(010) [101]

The elastic strain energy stored in a material due to presence of a dislocation is proportional to the product of Burgers vector $\vec{b}$ and bulk modulus G. For isotropic materials it follows that the strain energy is smallest for dislocations with the shortest Burgervectors- and those are the dislocations that will be formed. LiFePO$_4$ however is not isotropic as has been shown recently by Maxisch and Ceder by applying first principles calculations (14). Using the elastic constants published by Maxisch we estimate qualitative differences between elastic strain fields associated with dislocations of the three <100> type Burgers vectors. The estimated products $G\vec{b}$ for the dislocations considered here are listed together with the values used for the elastic moduli in the direction of the Burgers vectors in table II.

Table II : Burgers vectors and magnitudes of elastic strain in LiFePO$_4$			
Burgers vector[*]	**magnitude of $\vec{b}$**	**Directional Bulk Moduli [14]**	**$G\vec{b}$**
[100]	10.33Å	207 GPa	214 N/m
[010]	6.01Å	459 GPa	276 N/m
[001]	4.70Å	279 GPa	131 N/m

It can be seen that a dislocation with a Burgers vector $\vec{b}$=[001] that is glissile in both (100) and (010) planes has the lowest amount of elastic stress associated with it. For dislocation glide the elastic stress needs to be overcome. Therefore from the standpoint of elastic energy of a dislocation the formation of cracks is favorable in both observed directions. A better judgment on the activated glide systems can be obtained by the superposition of misfit stresses between two phases with elastic stress of dislocation lines as has been shown in precipitation hardened alloys (15).

Finally looking at the particle geometry of the LiFePO$_4$ powders used in both studies (sol gel versus hydrothermal) one may speculate that in case of the plate like particles having [010] surface normals cracks between (010) planes cannot be seen in transmission. On the other hand particles synthesized by the sol gel method have an arbitrary orientation of surface planes, which makes it more likely to observe both: cracks between (010) and between (100) planes. A closer look into Fig. 2a shows that perpendicular to the cracks between (010) planes smaller crack are observed. From the indices in this zone axis these smaller cracks are roughly between (701) planes which are at an angle of 3.71° to (100) planes.

Summary

We investigated carbon coated LiFePO$_4$ subjected to charge discharge cycling by transmission electron microscopy. Our results show that the carbon surface layer produced by our method withstood the cycling and was fully intact after over 100 charge discharge cycles. Micro cracks have been observed independently of the applied discharge rate. The surface orientation of the cracks observed in this study differs from the orientation of cracks observed in other studies. However considerations of the

---

[*] Burgers vectors of <110> type are not considered here for a lack of data on the elastic constants in these directions.

microstructure and elastic strain energy due to dislocations within the particles show that both orientations are feasible. The particle geometry of the delithiated particles suggests that only cracks parallel to the incident electron beam are visible in transmission electron microscopy while those perpendicular to the beam would not be detected if they were present.

Acknowledgments

References

1. A.K. Padhi, K.S. Nanjundaswami, and J.B. Goodenough, *J. Electrochem. Soc.*, **144**(4): p. 1188-1194, (1997).
2. D. Morgan, A. Van der Ven, and G. Ceder, *Electrochem. and Solid State letters*, **7**(2): p. A30-A32, (2004).
3. O. Haas, A. Deb, E.J. Cairns, and A. Wokaun, *Journal of the Electrochemical Society*, **152**(1): p. A191-A196, (2005).
4. A. Yamada, S.-Y. Chung, and K. Hinokuma, *Journal of the Electrochemical Society*, **148**(3): p. A224-A229, (2001).
5. N. Ravet, J.B. Goodenough, S. Besner, M. Simoneau, P. Hovington, and M. Armand. in *The Electrochemical Society and the Electrochemical Society of Japan Meeting*. 1999. Honolulu.
6. Z. Chen and J.R. Dahn, *Journal of the Electrochemical Society*, **140**(9): p. A1184-A1189, (2002).
7. K. Zaghib, J. Shim, A. Guerfi, P. Charest, and K. Striebel, *Electrochemical and Solid State Letters*, **8**(4): p. A207-A210, (2005).
8. F. Croce, A.D. Epifanio, J. Hassoun, A. Deptula, T. Olczac, and B. Scrosati, *Electrochemical and Solid State Letters*, **5**(3): p. A47-A50, (2002).
9. M.M. Doeff, Y. Hu, F. McLarnon, and R. Kostecki,. *Electrochemical and Solid State Letters*, **6**(10): p. A207-A209, (2003).
10. H. Gabrisch, J.D. Wilcox, and M.M. Doeff, *Electrochem. and Solid State letters*, **9**(6): p. A360-A363, (2006).
11. G. Chen, X. Song, and T.J. Richardson, *Electrochemical and Solid State letters*, **9**(6): p. A295-A298, (2006).
12. L. Laffont, C. Delacourt, P. Gibot, M. Yue, P. Kooyman, C. Masquelier, and J.M. Tarascon, *Chem. Mater.*: published on the web 10/24/2006, (2006).
13. D. Wang, X. Wu, Z. Wang, and L. Chen, *Journal of Power Sources*, **140**: p. 125-128, (2005).
14. T. Maxisch and G. Ceder, *Physical Review B*, **73**: p. 174112, (2006).
15. H. Gabrisch and D. Mukherji,. *Acta Materialia*, **48**: p. 3157-3167, (2000).